Physiological Measurement

IPEM Institute of Physics and Engineering in Medicine

ACCEPTED MANUSCRIPT

Photoplethysmography in dogs and cats: a selection of alternative measurement sites for pet monitor

To cite this article before publication: Blaž Cugmas *et al* 2018 *Physiol. Meas.* in press https://doi.org/10.1088/1361-6579/aaf433

IOP Publishing Journal Title
Journal **XX** (XXXX) XXXXXX https://doi.org/XXXX/XXXX

Photoplethysmography in dogs and cats: a selection of alternative measurement sites for pet monitor

Blaž Cugmas[1], Eva Štruc[2], Jānis Spīgulis[1]

[1] Biophotonics Laboratory, Institute of Atomic Physics and Spectroscopy, University of Latvia, 19 Raina Blvd., LV-1586, Riga, Latvia
[2] Animal Health Centre (Dzīvnieku veselības centrs), F. Candera Str. 4, LV-1046, Riga, Latvia

E-mail: blaz.cugmas@lu.lv

Abstract

Objective: Photoplethysmography (PPG) is an increasingly popular health and well-being tool for monitoring heart rate and oxygen saturation. Due to pigmentation and hairiness of dogs and cats, a pulse oximeter is routinely placed solely on the tongue. As this approach is feasible only for the pet monitor use during surgical procedures, we investigate PPG signal quality on several other measurement sites that would be better tolerated by conscious animals.
Approach: Acquired PPG signals are analyzed by four signal quality indices (SQI): mean baseline, signal power, kurtosis, and tolerance score.
Main Results: In dogs, the metacarpus and tail can substitute for oral pulse oximeter placement since both measurement sites exhibited high PPG signal kurtosis and were considered well-tolerated. In cats, the digit could be used with some limitations.
Significance: Pet monitors with pulse oximeter probes adjusted to promising measurement sites, could enable veterinarians and owners to monitor animals when fully awake.

Keywords: photoplethysmography, pulse oximeter, oxygen saturation, signal quality index, motion artifact, heart rate, pet monitor, veterinary medicine

1. Introduction

Measuring pulse rate (PR) and blood oxygenation (also peripheral oxygen saturation, SpO2) is a common monitoring procedure in veterinary medicine which gives important information about the patient's cardiovascular and respiratory systems. It can be performed as a part of physical examination (ASAVA 2013), surgical procedure (Bednarski *et al* 2011) or intensive care treatment (Humm and Kellett-Gregory 2016). In addition to veterinary professionals, pet owners are also becoming interested in painless and stress-free monitoring of their animals. This trend is reflected in the pet market where gadget devices for monitoring the canine or feline location and activity are on the rise (Weiss *et al* 2013).

Measuring PR and SpO2 can be done by the same optical probe which is based on the pulse oximetry sensor comprising continuously emitting light sources. The probe first emits and then, by the form of design, receives either the transmitted (e.g., on finger, tongue) or the reflected (e.g., on tail) red and infrared (IR) light (Allen 2007). If the acquired data is evaluated in time from a single spectral band, the technique is generally called photoplethysmography (PPG). On the other hand, pulse oximetry is based on comparing red and IR PPG signal baselines. The acquired PPG signal consists of non-pulsatile (DC) and pulsatile (AC) components. A baseline of PPG signal (i.e., non-pulsatile DC) reflects the collective light absorption due to blood and other tissues while the pulsatile

PPG component (AC) is a consequence of local blood volume changes in accordance with the cardiac cycle.

In humans, PPG is one of the most popular monitoring tool (Orphanidou 2018) since the device is small, reliable and low-cost. In addition to PR and SpO2, PPG is also used to monitor blood pressure, cardiac output, and the respiration rate, to detect various vascular diseases (Erts *et al* 2005, Karlen *et al* 2012, Bartels and Thiele 2015) and to assess regional anesthesia efficiency (Nijboer and Dorlas 1985, Rubins *et al* 2010). PPG probes are normally placed on fingertips for direct bedside monitoring. Recently, imaging PPG (iPPG) has become increasingly valuable since the PPG signals can be obtained from a camera or a mobile phone video (Huelsbusch and Blazek 2002, Jonathan and Leahy 2010, Remer and Bilenca 2015). It was shown that the PPG pulse varies significantly among measurement sites such as fingertips, toes, and ears (Allen 2007, Spigulis 2005). This phenomenon probably occurs due to differences in the cutaneous blood supply of the different anatomic regions (Maeda *et al* 2011). In addition to the anatomical differences of measurement sites, various physiological conditions can affect the PPG pulse (Alian and Shelley 2014). The amplitude of the AC component normally increases when vasodilatation occurs (e.g., regional anesthetic blocks, sepsis), but decreases with vasoconstriction (e.g., stress, cold) or with tissue congestion.

One of the biggest challenges when applying PPG in practice is signal quality (Orphanidou 2018). Patient movements (Krishnan *et al* 2010), ambient light (Allen 2007), and low peripheral perfusion (Karlen *et al* 2012) may all contribute to signal artifacts or to a weak PPG pulse in general. Consequently, many signal quality indices (SQI) have been employed for the assessment of PPG signal quality. SQI are various feature extraction methods (Elgendi 2016) which indicate a capability of pulse peaks and simple arrhythmias detection from a specific PPG signal. Furthermore, some SQI offer a detailed analysis thus providing more diagnostic value (Orphanidou 2018).

Since canine and feline anatomy and physiology are different, current human PPG measuring procedures and devices are not suitable for the use in pets. For example, the popular finger clips cannot be placed on canine or feline digit due to the presence of claws and pads. Furthermore, animal skin can be significantly more pigmented and hairy. Therefore, PPG probes are routinely attached only on the tongue when an animal is unconscious (e.g. during the surgical procedures). Otherwise, veterinarians have to improvise by placing the sensor on other low-pigmented measurement sites such as lip, vulva or prepuce (Humm and Kellett-Gregory 2016). According to our experience, these highly sensitive measurement sites are poorly tolerated in conscious animals as well.

Some of the recent animal PPG probe designs can be placed on other measurement sites like tail, but they have not been clinically validated yet. Moreover, the PPG technique has not been systematically studied or employed in the veterinary sciences. To the best of our knowledge, there have been only a few studies with PPG as a marginal method for canine health monitoring (Brugarolas *et al* 2014) or for analyzing perfusion and blood pressure (Binns Sarah H. *et al* 1995, Garcia-Granero *et al* 2003). Therefore, our motivation was to systematically evaluate the use of PPG in dogs and cats, starting with the analysis of alternative measurement sites which would complement the poorly tolerated oral probe. The aim of this first study was to find alternative measurement sites on the body surface which would be tolerated by conscious animals. PPG signal from the proposed sites were evaluated with four SQI and then compared to the existing oral measurement site. We propose that these findings would facilitate pet monitor use in dogs and cats.

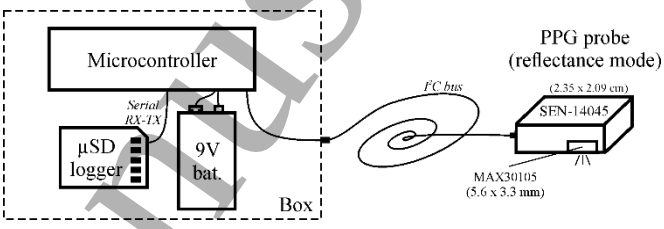

Figure 1. Diagram of the PPG device.

2. Material and methods

2.1 PPG Device

We built a small and portable custom-made PPG device (Figure 1) which was placed next to the animal without any additional holding equipment. The device, powered by a 9 V battery, worked in the reflectance mode. The pulse oximetry sensor MAX30105 (Maxim Integrated, USA) was integrated on the commercially available breakout board (2.35 cm x 2.06 cm, SEN-14045, SparkFun Electronics, USA). The optical sensor comprised three LEDs: green (peak wavelength – PW = 537 nm, full width at half maximum – FWHM = 35 nm), red (PW = 660 nm, FWHM = 20 nm) and near-infrared (IR) (PW = 880 nm, FWHM = 30 nm). The sensor was connected via serial I^2C bus to the microcontroller (Pro Micro 5V/16MHz, SparkFun Electronics) by an insulated and flexible cable in order to reach all measurement sites. Acquired data was stored via Arduino serial communication on a micro SD card (DEV-13712, SparkFun Electronics).

2.2 Animals and measurements

According to the national laws and European directive 2010/63/EU, the work was approved by the Latvian Food and

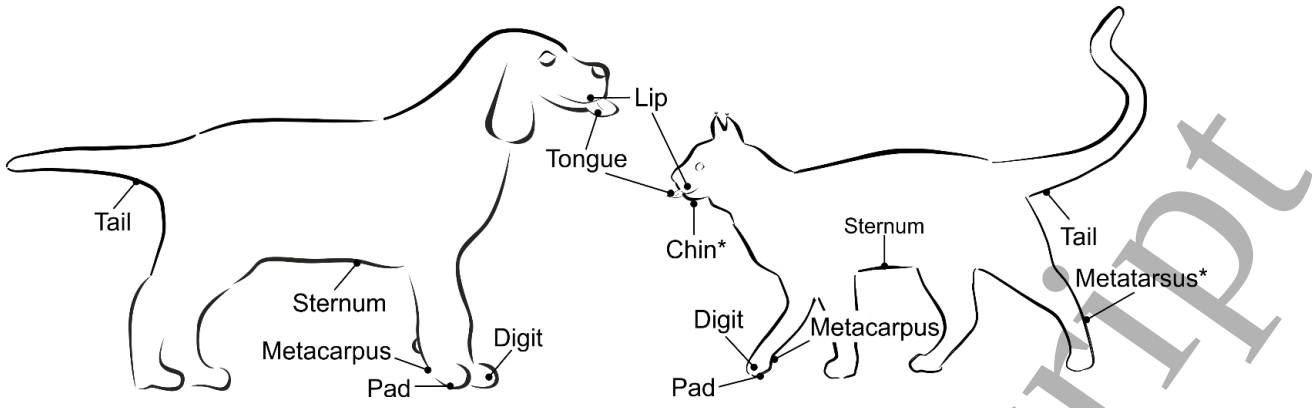

Figure 2. Investigated measurement sites (the sites with * were investigated only in cats).

Table 1. Measurement sites investigated in dogs and cats.

Short name	Precise location
Tongue	on the tongue
Lip	on the oral side of the upper lip, near the canine tooth
Metacarpus[a)]	in the palmar metacarpal region between the carpal and metacarpal pad
Pad	on the metacarpal pad
Digit	on the lateral side of the second digit of the front leg
Tail	on the ventral side of the tail, close to its base
Sternum	above the sternum's xiphoid process
Chin[b)]	on the chin
Metatarsus[a),b)]	in the plantar metatarsal region

[a)]Abbreviations Carpus and Tarsus are utilized in Table 4 and Figures 4, 5, and 8
[b)]Measurement sites investigated only in cats.

Veterinary Service, and the owner's written permission was collected.

Eleven dogs and ten cats of various ages and sizes were enrolled in the study. All PPG measurements were taken by the same operator during a scheduled dental cleaning procedure performed under general anesthesia. Seven measurement sites were investigated in the dogs and nine in the cats (Figure 2, Table 1). Where the hair obstructed the good optical coupling between the sensor and the skin, the measurement site was shaved (with an area up to one cm^2) before the signal acquisition. The sensor was then gently pressed against the tissue, and the PPG signal was recorded for 20-30 seconds. For each measurement, the data were manually checked for abnormalities (artifacts) in signal baseline which occurred if an animal had to be moved or if personnel mistakenly touched the measurement equipment. The corrupted sections were removed from further analysis to ensure approximately 10 seconds of unspoiled and clear PPG signal. Parallel to each PPG acquisition, heart rate (HR) was estimated by auscultation by the anesthesiologist.

2.3 Signal processing

After data acquisition, all raw PPG signals ($x_{raw}(t)$) were normalized separately for each channel with the reference signal baseline B_{white} acquired on the standard white color patch of ColorChecker Classic (X-rite, Michigan, the USA):

$$x(t) = \frac{x_{raw}(t)}{B_{white}}. \quad (1)$$

Normalized signals were arranged into groups according to measurement sites and animal species. To investigate possible alternative measurement sites, four PPG features (SQI) were extracted, matching four criteria for the evaluation of measurement site suitability.

First, a typical signal baseline (B) for a specific measurement site was calculated as a median of signal baselines (i.e. DC components or signal means $\bar{x}$):

$$B = median(\bar{x}_i), i = 1 \dots n, \quad (2)$$

where n is a number of measurements on a specific measurement site. Typical baseline B indicated measurement sites with high light absorption due to pigmentation and hairiness.

Secondly, the PPG signal power (P_{PPG}) (Elgendi 2016) in the HR-limited frequency range was estimated for each measurement with the *bandpower* function (Matlab R2015a, MathWorks Inc, USA) as:

$$P_{PPG} = \int_{HR-0.5Hz}^{HR+0.5Hz} S_x(f)df, \quad (3)$$

where S_x represents a power spectrum of the normalized PPG signal $x(t)$. Frequency range was limited with a deviation of 0.5 Hz around the measured heart rate (HR) to keep the SQI resilient to small HR time deviations. A typical signal power (P) for a specific measurement site was calculated as a median of signal powers (P_{PPG}) in the same manner as in Eq. 2.

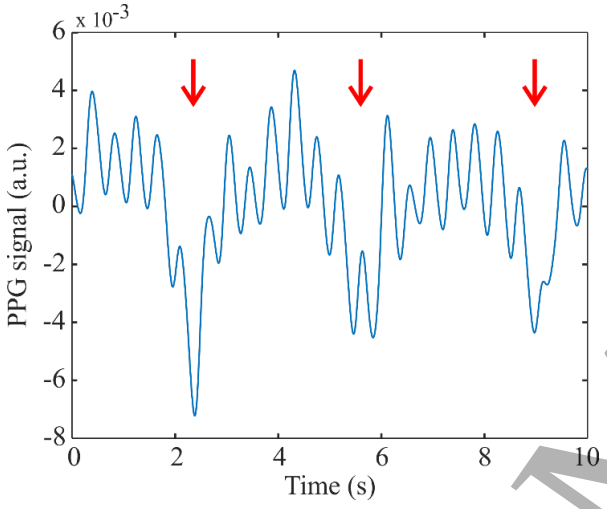

Figure 3. Filtered canine PPG signal $x(t)$ (band-pass filter frequencies of 0.2 Hz and 3 Hz, pulse rate (PR) is 137 bpm) from measurement site above the sternum where the respiration (19 breaths per minute) impact could be seen (red arrows). Arbitrary units (a.u.) were obtained with the normalization against the white reference.

In addition to PPG signal, the signal power (P_{PPG}) also contains noise with matching frequency range (e.g., due to motion or ambient light artifacts). Thus, kurtosis (k_{PPG}) was selected as the third SQI. Kurtosis describes the shape of probability distribution around the mean (Orphanidou 2018, Elgendi 2016). In our case, the shape of the PPG power spectrum (S_x') was studied. The spectrum with a sharp peak will have higher kurtosis value comparing to the noisy signal kurtosis. Therefore, kurtosis can be applied as an indicator of PPG signal quality. Before the kurtosis calculation, low (e.g., due to respiration) and high-frequency components (e.g., due to signal harmonics) were filtered out. In humans, the examined PPG frequency range is normally between 0.5 and 2 Hz (Orphanidou 2018). Since HR of animals is higher, the selected range was between 1-3 Hz for dogs and 1.25-3.6 Hz for cats. Kurtosis (k_{PPG}) was estimated with the *kurtosis* function (Matlab R2015a) as (Orphanidou 2018, Krishnan *et al* 2010, Elgendi 2016):

$$k_{PPG} = \frac{E(S-\mu)^4}{\sigma^4}, \quad (4)$$

where μ is the mean of S, E is the estimated value of $E(t)$, and σ is the standard deviation. A typical kurtosis (k) for a specific measurement site was calculated as a median of signal kurtoses (k_{PPG}).

The fourth SQI was a tolerance score estimated independently by three clinical veterinarians. Since animals were under general anesthesia, the tolerance score could not be based on the animal defensive behavior (Gomart *et al* 2014). Instead, the veterinarians were told to associate PPG measurements with the intravenous therapy in conscious patients due to similarities in shaving and line placement. Analogously, as the animal movements could jeopardize fluid flow, quality of PPG signal could be deteriorated.

Separately for dogs and cats, veterinarian arranged measurements sites from the best to the worst tolerated. According to the arrangement, each measurements site received the tolerance score (ranging between 1-7 and 1-9 for dogs and cats, respectively). In the end, a final tolerance score was calculated as an average of all three scores.

Collectively, four SQI were estimated for each measurement site:

1. typical signal baseline (B),
2. typical signal power (P),
3. typical kurtosis (k),
4. tolerance score given by the veterinarians.

Most of the medical and veterinary PPG monitors utilize only the IR channel (Alian and Shelley 2014), thus, the first three SQI (B, P, and k) were calculated solely from IR data. Measurement sites were arranged from the best to the worst for each SQI. Finally, the measurement site with the lowest sum of placings was considered the most suitable.

Since this study was a part of the H2020 Open Research Data Pilot, the original data is located on the Zenodo under DOI identifier *10.5281/zenodo.1296214*.

3. Results and discussion

In 11 dogs, seven measurement sites were evaluated. Seven PPG measurements on pads and three on the sternum did not exhibit 10 seconds of an unspoiled and clear PPG signal. Therefore, these data were excluded from further processing. In ten cats, nine measurement sites were tested. The number of excluded PPG signal measurements was higher, i.e. 19. Most of the exclusions happened with the measurements on

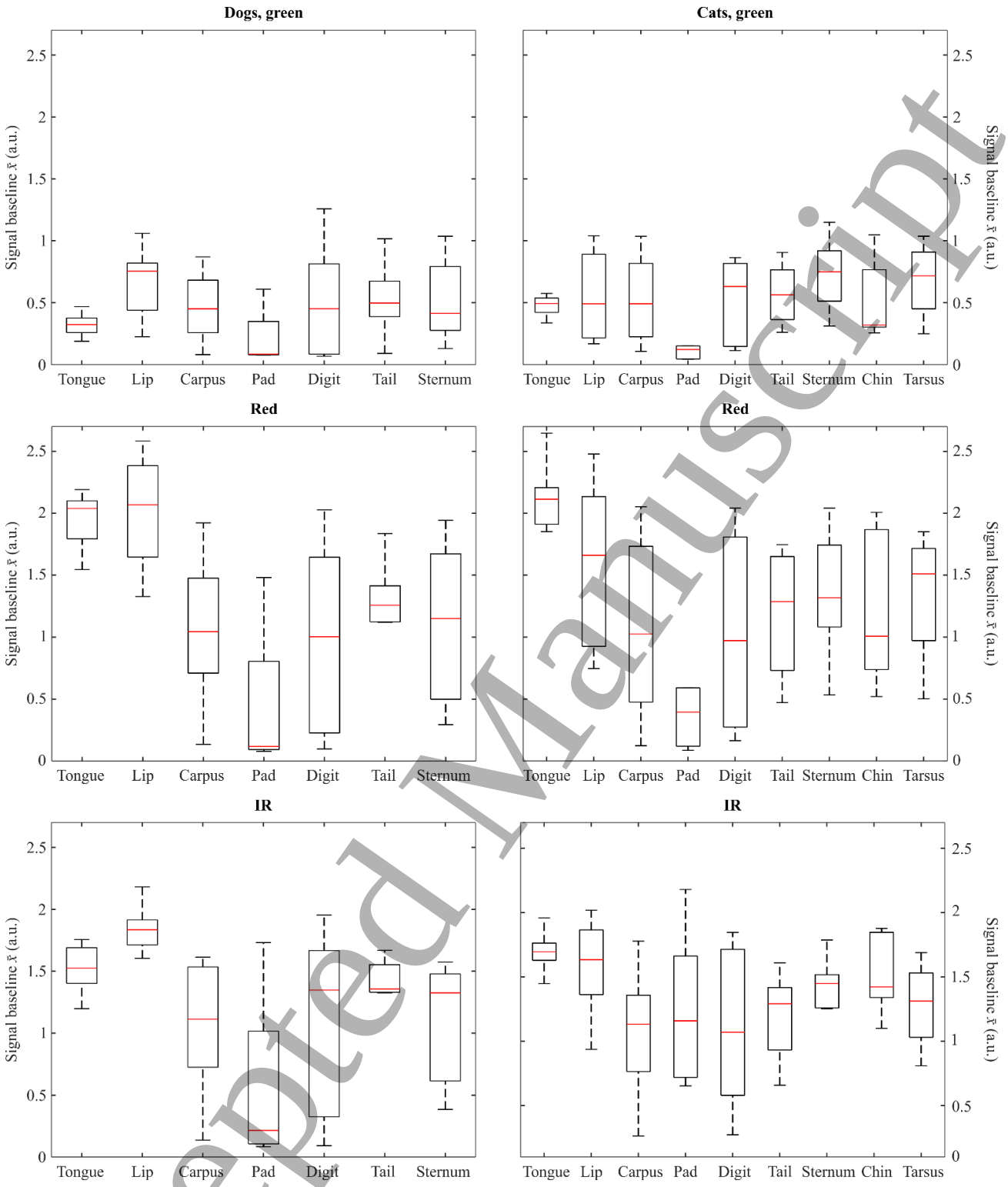

Figure 5. Figure 4. Baselines (i.e. DC component, $\bar{x}$) for green, red and IR PPG signals. Red line represents the median, i.e. typical signal baseline (B). The bottom and top box edges indicate the 25th and 75th percentiles, respectively. Both whiskers present the extreme data points.

Table 2. Canine PPG signal power (P_{PPG}) and kurtosis (k_{PPG}): median value (also known as typical signal power (P) or kurtosis (k)) with 5th and 95th percentiles in squared brackets.

	Green		Red		IR	
	P_{PPG} (10^{-7})	k_{PPG}	P_{PPG} (10^{-7})	k_{PPG}	P_{PPG} (10^{-7})	k_{PPG}
Tongue	2.19 [0.1 – 42.6]	7.69 [4.2 – 70.8]	2.87 [0.3 – 145.2]	5.60 [3.8 – 23.5]	4.26 [1.6 – 376.9]	10.78 [4.2 – 42.1]
Lip	3.06 [0.4 – 287.2]	8.59 [3.7 – 15.6]	2.79 [0.5 – 52.7]	6.12 [2.8 – 29.8]	4.86 [0.3 – 371.6]	10.46 [4.7 – 39.8]
Metacarpus	2.35 [0.2 – 40.7]	11.90 [5.2 – 62.5]	1.17 [0.0 – 157.5]	11.44 [3.5 – 63.6]	6.60 [0.1 – 1286.6]	20.59 [5.7 – 65.4]
Pad	0.07 [0.0 – 3.5]	5.17 [3.2 – 18.4]	0.00 [0.0 – 2.0]	4.35 [3.5 – 35.2]	0.04 [0.0 – 16.4]	6.15 [4.4 – 51.6]
Digit	4.29 [0.2 – 41.9]	10.12 [5.1 – 60.4]	4.63 [0.0 – 47.8]	6.09 [5.2 – 35.5]	3.24 [0.0 – 46.4]	6.19 [4.9 – 50.8]
Tail	0.22 [0.1 – 2.8]	5.78 [3.2 – 16.9]	0.40 [0.0 – 4.0]	6.94 [5.2 – 26.7]	2.24 [0.0 – 17.7]	18.4 [5.1 – 44.2]
Sternum	1.17 [0.1 – 9.4]	6.34 [3.6 – 20.8]	0.53 [0.0 – 83.8]	4.18 [2.6 – 19.3]	0.40 [0.1 – 214.9]	6.68 [3.1 – 15.1]

Table 3. Feline PPG signal power (P_{PPG}) and kurtosis (k_{PPG}): median value (also known as typical signal power (P) or kurtosis (k)) with 5th and 95th percentiles in squared brackets.

	Green		Red		IR	
	P_{PPG} (10^{-7})	k_{PPG}	P_{PPG} (10^{-7})	k_{PPG}	P_{PPG} (10^{-7})	k_{PPG}
Tongue	1.73 [0.2 – 21.8]	6.87 [3.5 – 32.2]	1.32 [0.2 – 30.1]	5.87 [3.1 – 29.4]	2.03 [0.9 – 133.6]	9.11 [3.4 – 66.4]
Lip	1.46 [0.1 – 3.1]	4.77 [2.7 – 21.6]	1.09 [0.3 – 22.5]	4.67 [2.9 – 10.3]	1.40 [0.1 – 14.0]	4.64 [3.2 – 13.4]
Metacarpus	0.77 [0.0 – 16.6]	6.45 [2.7 – 29.7]	0.34 [0.0 – 2.5]	5.71 [3.5 – 14.1]	0.12 [0.0 – 2.8]	4.60 [2.8 – 33.3]
Pad	0.06 [0.0 – 2.3]	4.80 [3.2 – 29.8]	0.01 [0.0 – 4.4]	3.36 [2.5 – 26.6]	0.09 [0.0 – 8.2]	16.29 [4.6 – 23.2]
Digit	3.11 [0.1 – 147.7]	7.64 [4.2 – 52.1]	2.00 [0.0 – 27.6]	12.11 [3.1 – 48.3]	2.24 [0.2 – 122.4]	14.15 [4.8 – 50.5]
Tail	2.44 [0.1 – 32.4]	5.30 [3.3 – 19.1]	0.66 [0.1 –4.9]	4.83 [3.5 – 14.4]	1.24 [0.2 –31.0]	6.51 [2.6 – 23.6]
Sternum	0.56 [0.1 – 2.8]	6.79 [3.3 – 14.8]	0.60 [0.0 – 1.4]	4.69 [2.3 – 11.9]	0.33 [0.1 – 2.1]	5.33 [2.6 – 31.2]
Chin	0.47 [0.1 – 2.8]	4.25 [3.7 – 13.7]	0.36 [0.1 – 0.8]	4.03 [2.7 – 11.7]	0.41 [0.1 – 1.0]	4.44 [2.8 – 7.0]
Metatarsus	1.22 [0.1 –3.5]	6.72 [2.9 – 9.6]	0.11 [0.0 – 0.4]	5.36 [2.7 – 43.7]	0.10 [0.0 – 0.4]	5.59 [3.3 – 58.4]

the pad, the sternum, and the metatarsus. The reason for the higher number of feline exclusions might be due to feline body size, which was on average much smaller than the canine. Consequently, it was harder to fix the PPG probe against the body surface and sample the desired area. In both, canine and feline cases, more exclusions occurred on the sternum where respiration introduced motion artifacts to PPG signal (Figure 3).

The baselines of PPG signals (i.e. DC components or signal means $\bar{x}$) were studied first (Figure 4). It was evident that the green light had been absorbed the most since its typical signal baselines (B) were around 0.5 a.u. (normalized against the

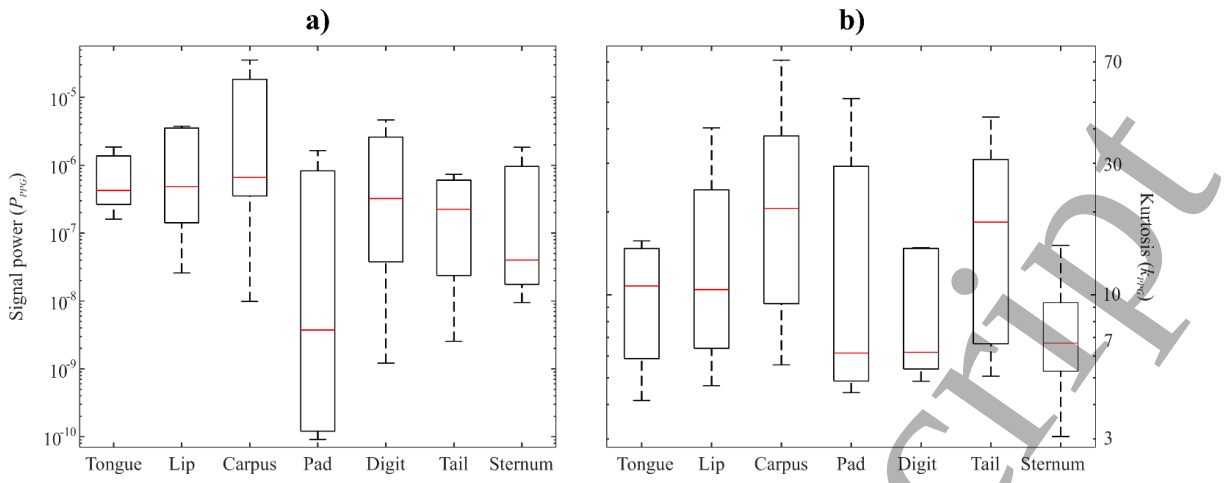

Figure 5. Canine IR PPG signal a) power (P_{PPG}) and b) kurtosis (k_{PPG}). Red lines represent median, i.e. typical signal power (P) or kurtosis (k). The bottom and top box edges indicate the 25th and 75th percentiles, respectively. Both whiskers present the extreme data points. P_{PPG} was calculated from $x(t)$ (Eq. 3, a.u. units).

white reference). On the other hand, the red and IR baselines were between 1 and 2 a.u. There were no obvious baseline differences between measurement sites with lower (e.g., tongue) or higher (e.g., metacarpus) melanin concentration. It can be speculated that due to the PPG sensor design and shallow green light penetration, the direct reflection from the surface was dominant over the diffuse component containing PPG signal.

On the other hand, the difference between nonpigmented and pigmented sites was evidently seen in baselines of red and IR PPG signals. The typical signal baseline on normally nonpigmented lips and tongue (i.e., mucosa) was higher than the baseline on the pigmented measurement sites (skin). The difference was even more evident with highly keratinized measurement sites such as the pads. Additionally, the differences in baseline between mucosa and skin were more apparent with the red light where the difference in baseline was around 50 %, compared with the difference of 29 % in the IR channel. This observation was expected since melanin has a higher absorption coefficient in the red than in the IR wavelength range. Furthermore, the baseline difference between mucosa and skin was larger in dogs (~46 %) than in cats (~33 %). That may be caused by darker, hairier and thicker canine skin.

Next, the signal power (P_{PPG}) and kurtosis (k_{PPG}) were analyzed (Tables 2 and 3). The tables include the data for all channels; however, the analysis, discussion, and figures focus solely on the IR channel (Alian and Shelley 2014).

In dogs, the highest signal power appeared on the metacarpus (Figure 5(a)) which was slightly greater than the

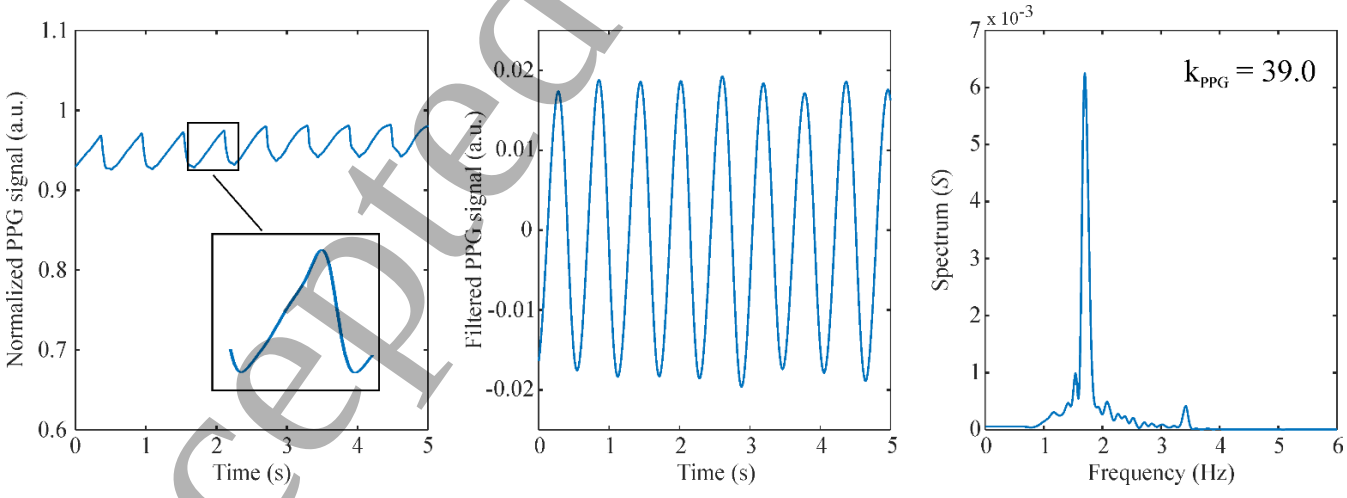

Figure 6. An example of good canine PPG signal (IR, metacarpus, PR = 101 bpm): normalized PPG signal ($x(t)$)* with one filtered PPG pulse, filtered PPG signal (band-pass filter frequencies of 1 Hz and 3 Hz) and its frequency spectrum (S) for kurtosis (k_{PPG}) estimation. *signal is not inverted; therefore, it is opposite to the blood volume changes.

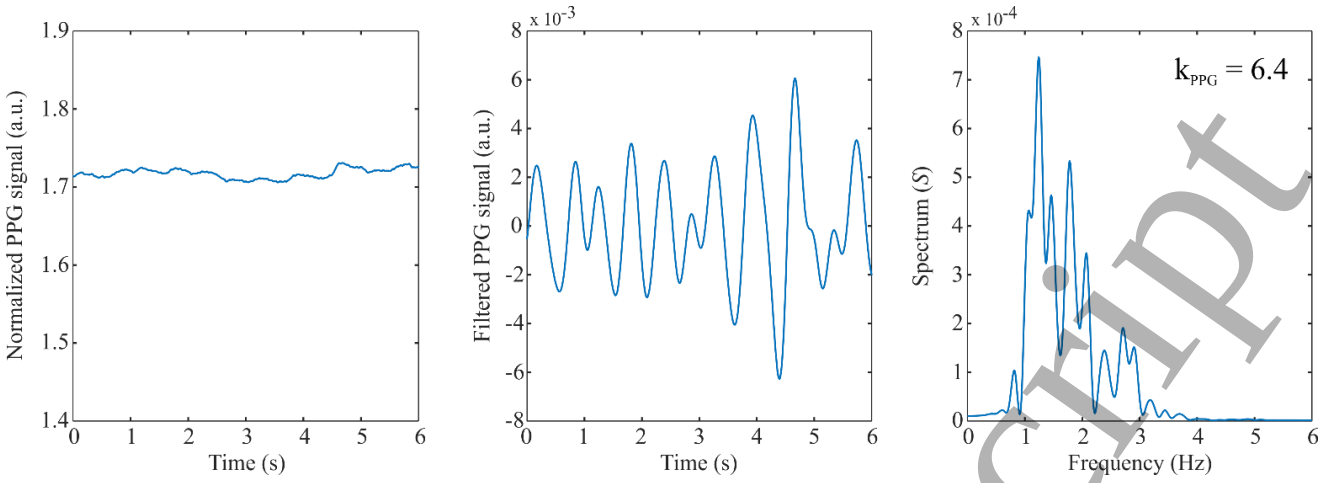

Figure 7**.** An example of poor canine PPG signal (IR, digit, PR = 116 bpm): normalized PPG signal ($x(t)$), filtered PPG signal (band-pass filter frequencies of 1 Hz and 3 Hz) and its frequency spectrum (S) for kurtosis (k_{PPG}) estimation.

P_{PPG} on the tongue and lips. In contrast, the P_{PPG} values on both mucosal sites were less dispersed. This points towards more stable measurements at these measurement sites. The tongue and lips are quite homogenous and include evenly perfused tissues. In contrast, the metacarpus region is diverse and includes larger blood vessels, muscles, tendons, and bones, making repeatable measurements challenging.

The weakest PPG pulse was recorded on the pads where P_{PPG} was on average two orders of magnitude lower than the PPG power of the metacarpus and mucosal sites. This phenomenon is predominantly related to the high absorbance of canine pads (Figure 4) which exhibit modified skin anatomy and morphology. It could be highlighted that canine pads have a thick, heavily pigmented, and avascular stratum corneum (i.e. the outermost layer) which can easily exceed the thickness of 2-3 mm (Ninomiya *et al* 2013). Additionally, the pad surface includes elongated spike-like conical papillae which probably cause the formation of an air layer between the sensor and the pad. In lightly pigmented skin, penetration depth of near-infrared (NIR) light is up to 12 mm (Kohen *et al* 1995, Bashkatov *et al* 2005). However, when the pigmentation is stronger, the mean penetration depth can decrease to 3 mm (Cugmas *et al* 2015) which is close to the stratum corneum thickness. Therefore, very little diffusely reflected light impacted by the underlying perfusion can be expected to be detected on the pads.

As with signal power, the metacarpus exhibited the highest typical kurtosis (k) of 20.59 (Figure 5(b)). On the other hand,

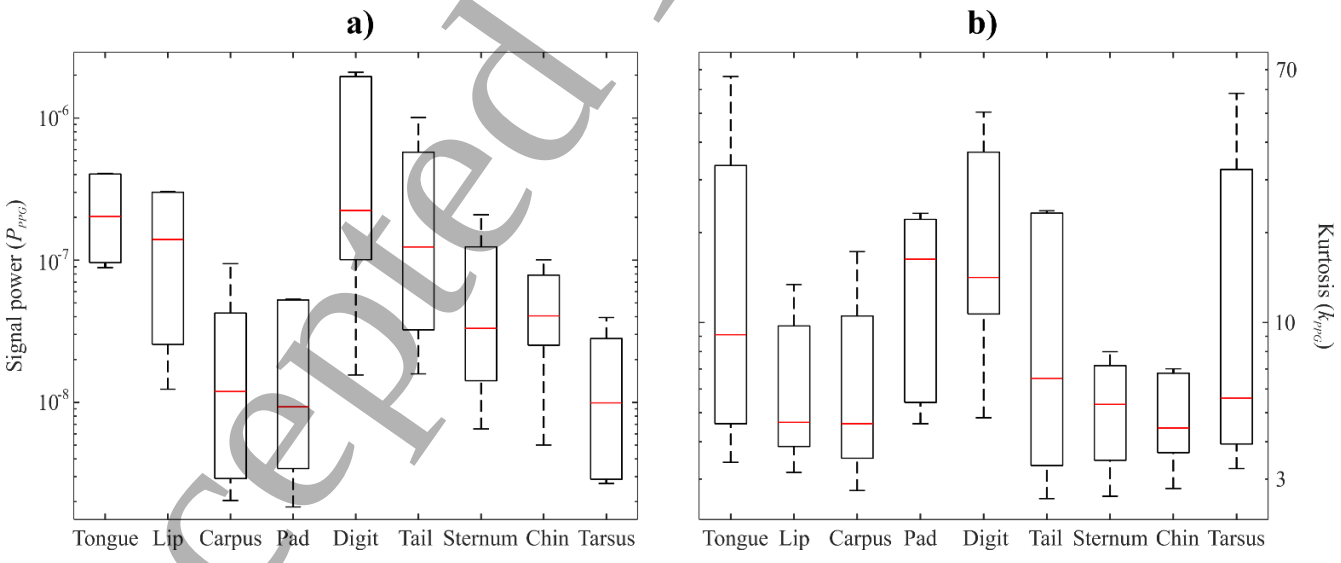

Figure 8. Feline IR PPG signal a) power (P_{PPG}) and b) kurtosis (k_{PPG}). Red lines represent median, i.e. typical signal power (P) or kurtosis (k). The bottom and top box edges indicate the 25th and 75th percentiles, respectively. Both whiskers present the extreme data points.

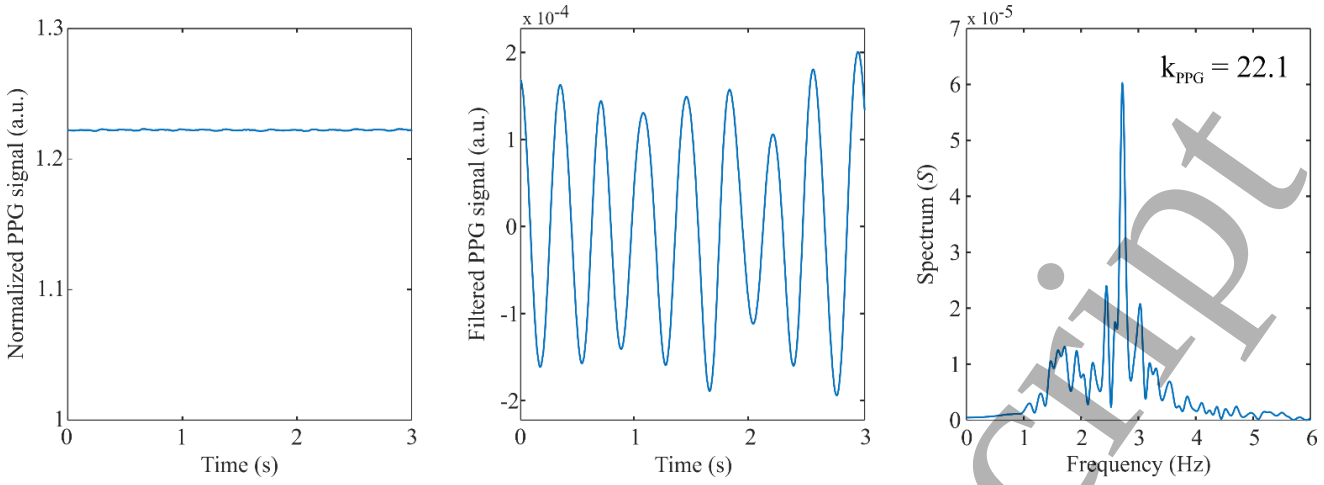

Figure 9. Feline PPG signal with low power and high kurtosis (IR, pad, PR = 163 bpm): normalized PPG signal ($x(t)$), filtered PPG signal (band-pass filter frequencies of 1.25 Hz and 3.6 Hz) and its frequency spectrum (S) with kurtosis (k_{PPG}).

kurtoses on the sternum, pads, and digit were just above 6, three and a half times less than the typical metacarpal kurtosis. Similar kurtosis ratios between good and poor PPG signals were also observed in a human study (Orphanidou 2018). An example of a good PPG signal with high kurtosis (k = 39.0) is shown in Figure 6. On the other hand, a poor PPG signal still allowed the estimation of pulse rate (PR) (Figure 7); but, the signal included many artifacts and, thus, its diagnostic value is questionable.

Apart from both mucosal measurement sites in cats, the highest P_{PPG} appeared on the digit and tail (Figure 8). In contrast, the signal power was low on the metacarpus, pads, and metatarsus. Despite this fact, some metatarsal PPG signals exhibited very high kurtosis (k_{PPG}) which would confirm our assumption above that sampling a desired vascular area in cats is challenging. Even a higher discrepancy between P_{PPG} and k_{PPG} was found on the pads where the PPG signal exhibited the highest typical kurtosis (k). Compared to dogs, feline pads have thinner stratum corneum and less pigmentation, and they do not have superficial papillae (Ninomiya *et al* 2013). It can be concluded that in the case of lightly pigmented pads, the quality of the acquired PPG signal is high, despite its low power (Figure 9).

For the final evaluation, the measurement sites were arranged from the best to the worst according to the four SQI: typical signal baseline (B), power (P), kurtosis (k), and tolerance score estimated by the veterinarians (Table 4). In dogs, the metacarpus (final sum = 10 points) performed superiorly compared to the other measurement sites, including the tongue (15 points), which is the only routinely used measurement site in veterinary practice. On the other hand, the metacarpal signal can have a low signal baseline (i.e. DC component) due to the possibility of pigmentation and hairiness. However, this did not affect the signal power (P_{PPG}) and kurtosis (k_{PPG}). The veterinarians in this study agreed that the PPG acquisition in the metacarpal region would be well-

Table 4. Measurement sites arranged according to the four SQI: typical signal baseline (B), typical signal power (P), typical kurtosis (k) and tolerance score given by veterinarians (*Vet Score*). All SQI scores were summed (*sum*) and listed in brackets. According to score sums, measurement sites were arranged from the most to the least suitable (*Final*).

	SQI	Tongue	Lip	Carpus	Pad	Digit	Tail	Sternum	Chin	Tarsus
Dogs	*B*	2	1	6	7	4	3	5	/	/
	P	3	2	1	7	4	5	6		
	k	3	4	1	6	7	2	5		
	Vet Score	7	6	2	5	4	3	1		
	Final (sum)	**4.** (15)	**2.** (13)	**1.** (10)	**7.** (25)	**6.** (19)	**2.** (13)	**5.** (17)		
Cats	*B*	1	2	8	7	9	6	4	3	5
	P	2	3	7	9	1	4	6	5	8
	k	3	7	8	1	2	4	6	9	5
	Vet Score	9	8	1	5	6	4	2	7	3
	Final (sum)	**1.** (15)	**5.** (20)	**8.** (24)	**7.** (22)	**2.** (18)	**2.** (18)	**2.** (18)	**8.** (24)	**6.** (21)

tolerated by the animals. In addition to both mucosal measurement sites, the tail also exhibited satisfactory results (13 points). Except for the signal power, all other parameters were notable. In the end, we should emphasize that veterinary PPG probes normally work in transmittance mode, but in our study, a reflectance probe was applied.

In cats, the tongue still performed the best (15 points). The measurement sites of the digit, tail and, sternum followed with the sum of 18 points. However, the sternum and the tail had low signal power and kurtosis (Figure 3). Therefore, the digit with high P_{PPG} and k_{PPG} could be used when an alternative measurement site is sought. As with canine metacarpus, the digit in cats exhibited low signal baseline (B) and tolerance score. Surprisingly, the feline metacarpus altogether performed the worst (24 points) due to very low signal power and kurtosis, despite the highest predicted tolerance score.

4. Conclusion

When the PPG signal is observed, a pet monitor could be applied on the metacarpus or the tail in the place of the tongue. Both of these measurement sites exhibited high PPG signal kurtosis, and they were considered well tolerated by the animals. On the other hand, the typical measurement site in cats (i.e., tongue) cannot be so easily replaced with another measurement site. Thus, if one has to apply pulse oximeter to a conscious cat, the digit could be used.

It should be noted that this study was performed on anesthetized animals. Placing a pulse oximeter to a conscious pet would additionally affect measurement site suitability. For example, motion artifacts due to animal movements and respiration (Fig. 3) can lower the PPG signal quality. In the future, the robustness of PPG on conscious animals should be tested.

In the future, new probes adjusted to the well-tolerated measurement sites could be developed and clinically applied to test their repeatability. Additionally, more specific PPG studies on pulse transit times (PTT), PPG pulse shape, etc. could be realized.

Acknowledgments

This project has received funding from the European Union's Horizon 2020 research and innovation programme under the Marie Skłodowska-Curie grant agreement No 745396 (DogSPEC). We would also like to express our gratitude to veterinarians Liene Dindone, Alla Olivrī, Aigars Briņķis, Solvita Buivide and all other personnel at Animal Health Centre (DVC) in Riga for all the help and technical support.

References

Alian A A and Shelley K H 2014 Photoplethysmography *Hemodynamic Monit. Devices* **28** 395–406

Allen J 2007 Photoplethysmography and its application in clinical physiological measurement *Physiol. Meas.* **28** R1

ASAVA 2013 Regular health check standards for dogs and cats Online: http://www.ava.com.au/asav/resources

Bartels K and Thiele R H 2015 Advances in photoplethysmography: beyond arterial oxygen saturation *Can. J. Anesth. Can. Anesth.* **62** 1313–28

Bashkatov A N, Genina E A, Kochubey V I and Tuchin V V 2005 Optical properties of human skin, subcutaneous and mucous tissues in the wavelength range from 400 to 2000 nm *J. Phys. -Appl. Phys.* **38** 2543–55

Bednarski R, Grimm K, Harvey R, Lukasik V M, Penn W S, Sargent B and Spelts K 2011 AAHA Anesthesia Guidelines for Dogs and Cats *J. Am. Anim. Hosp. Assoc.* **47** 377–85

Binns Sarah H., Sisson D. David, Buoscio Dana A. and Schaeffer David J. 1995 Doppler Ultrasonographic, Oscillometric Sphygmomanometric, and Photoplethysmographic Techniques for Noninvasive Blood Pressure Measurement in Anesthetized Cats *J. Vet. Intern. Med.* **9** 405–14

Brugarolas R, Dieffenderfer J, Walker K, Wagner A, Sherman B, Roberts D and Bozkurt A 2014 Wearable wireless biophotonic and biopotential sensors for canine health monitoring *IEEE SENSORS 2014* 2203–6

Cugmas B, Plavec T, Bregar M, Naglič P, Pernuš F, Likar B and Bürmen M 2015 Detection of canine skin and subcutaneous tumors by visible and near-infrared diffuse reflectance spectroscopy *J. Biomed. Opt.* **20** 037003

Elgendi M 2016 Optimal Signal Quality Index for Photoplethysmogram Signals ed G-J Wang *Bioengineering* **3** 21

Erts R, Spigulis J, Kukulis I and Ozols M 2005 Bilateral photoplethysmography studies of the leg arterial stenosis *Physiol. Meas.* **26** 865

Garcia-Granero E, Garcia S A, Alos R, Calvete J, Flor-Lorente B, Willatt J and Lledo S 2003 Use of Photoplethysmography to Determine Gastrointestinal Perfusion Pressure: An Experimental Canine Model *Dig. Surg.* **20** 222–8

Gomart S B, Allerton F J W and Gommeren K 2014 Accuracy of different temperature reading techniques and associated stress response in hospitalized dogs *J. Vet. Emerg. Crit. Care* **24** 279–85

Huelsbusch M and Blazek V 2002 Contactless mapping of rhythmical phenomena in tissue perfusion using PPGI *Proc. SPIE 4683* 4683–8

Humm K and Kellett-Gregory L 2016 Monitoring small animal patients in the intensive care unit *In Pract.* **38** 12

Jonathan E and Leahy M J 2010 Cellular phone-based photoplethysmographic imaging *J. Biophotonics* **4** 293–6

Karlen W, Kobayashi K, Ansermino J and Dumont G 2012 Photoplethysmogram signal quality estimation using repeated Gaussian filters and cross-correlation *Physiol. Meas.* **33** 1617

Kohen E, Santus R and Hirschberg J G 1995 *Photobiology* (San Diego: Elsevier Science)

Krishnan R, Natarajan B and Warren S 2010 Two-Stage Approach for Detection and Reduction of Motion Artifacts in Photoplethysmographic Data *IEEE Trans. Biomed. Eng.* **57** 1867–76

Maeda Y, Sekine M and Tamura T 2011 Relationship Between Measurement Site and Motion Artifacts in Wearable Reflected Photoplethysmography *J. Med. Syst.* **35** 969–76

Nijboer J A and Dorlas J C 1985 Comparison of plethysmograms taken from finger and pinna during anaesthesia *Br. J. Anaesth.* **57** 531–4

Ninomiya H, Yamazaki K and Inomata T 2013 Comparative Anatomy of the Vasculature of the Dog (Canis familiaris) and Domestic Cat (Felis catus) Paw Pad *Open J. Vet. Med.* **3** 5

Orphanidou C 2018 *Signal Quality Assessment in Physiological Monitoring: State of the Art and Practical Considerations* (Cham, Switzerland: Springer International Publishing)

Remer I and Bilenca A 2015 Laser speckle spatiotemporal variance analysis for noninvasive widefield measurements of blood pulsation and pulse rate on a camera-phone *J. Biophotonics* **8** 902–7

Rubins U, Miscuks A, Rubenis O, Erts R and Grabovskis A 2010 The analysis of blood flow changes under local anesthetic input using non-contact technique *3rd International Conference on Biomedical Engineering and Informatics*

Spigulis J 2005 Optical noninvasive monitoring of skin blood pulsations *Appl. Opt.* **44** 1850–7

Weiss G M, Nathan A, Kropp J B and Lockhart J W 2013 WagTag: a dog collar accessory for monitoring canine activity levels *ACM conference on Pervasive and ubiquitous computing adjunct publication*